PHYSICAL REVIEW A **106**, L021501 (2022)

Letter

# Correlation-driven charge migration as an initial step of the dynamics in correlation bands

Victor Despré[*] and Alexander I. Kuleff[†]
*Theoretische Chemie, PCI, Universität Heidelberg, Im Neuenheimer Feld 229, D-69120 Heidelberg, Germany*

(Received 26 October 2021; accepted 18 July 2022; published 11 August 2022)

We present quantum dynamics calculations showing that the electron-correlation-driven charge migration occurring in the correlation band of ionized molecules can lead to a redistribution of the charge which increases the stability of the system. These calculations offer an interpretation of recent experimental results obtained for adenine for which the stabilization induced by the electron-correlation-driven charge migration leads to a modification of the fragmentation pattern of the molecule after subsequent ionization. We argue that this charge-migration-induced stabilization is a general mechanism and discuss its implications for the development of attochemistry and how it can be understood in the context of the ultrafast, nonadiabatic relaxation taking place in highly excited molecular cations.

DOI: 10.1103/PhysRevA.106.L021501

The development of ultrafast technology allows one nowadays to study electron dynamics in their intrinsic time scale [1]. The observation of pure electron dynamics occurring after photoionization of molecular systems [2–4] is a first step towards the realization of attochemistry, namely, the possibility to control the reactivity of a molecular system by acting only on its electronic degrees of freedom. These dynamics, referred to as charge migration, have been intensively studied theoretically in the last two decades (see, e.g., Refs. [5–19]), showing that charge migration is a rich phenomenon, with many facets that are rather characteristic for the investigated molecule. A mechanism of particular interest in this context is the so-called correlation-driven charge migration [6,20], in which the hole charge created by ionization can migrate throughout the molecule on a few-femtosecond time scale. These charge dynamics appear as a result of the population of specific coherent superpositions of electronic states upon ionization, determined by the electron-correlation effects in the molecule. Despite the great interest, experimental study of the correlation-driven charge migration is still very challenging, and the phenomenon has not been directly observed yet. One of the reasons is that even at fixed nuclei, the zero-point spread of the nuclear wave packet causes an electronic dephasing that puts the pure electronic charge migration quickly to an end [21,22]. Moreover, the coupling to the nuclear motion may destroy the initially created electronic coherence extremely fast. Decoherence times of less than 3 fs have been predicted for certain molecules and electronic states [23,24]. It has to be noted, however, that longer-lived electronic coherences have also been predicted for polyatomics [21,25], offering suitable systems to study the correlation-driven charge-migration phenomenon.

Very recently, in a pioneering experiment, Calegari and co-workers where able to identify a sub-3-fs pure electron dynamics in adenine [26]. This dynamics triggered by an XUV ionization is observed through a positive delay in the appearance of the parent-dication signal after a second ionization of the adenine with a near-infrared (NIR) pulse in a pump-probe scheme. As the analysis showed that only two NIR photons are absorbed, the probed dynamics have to take place a few eV below the double-ionization threshold, i.e., in the correlation band of adenine. The electron dynamics thus causes a delay in the onset of the nonadiabatic relaxation in the correlation band of the system. The characteristic correlation-band relaxation dynamics were recently identified in a series of polycyclic aromatic hydrocarbon molecules [27], and they also allowed previously published results [28–30] to be interpreted. Correlation bands [31] exist in all molecular systems of sufficient size and appear in their ionization spectra as a large increase in the density of states just below the double-ionization threshold, due to the electron-correlation-induced breakdown of the molecular-orbital picture [32]. It was shown [27] that the relaxation in correlation bands follows a characteristic scaling law for a given family of molecular systems of increasing size, competing with the simultaneously occurring redistribution of the energy among the different vibrational degrees of freedom [33]. In the context of attochemistry, the identification of pure electron dynamics preceding the universal nonadiabatic relaxation in the correlation band is very important, as such an event sequence may offer a possibility to control the overall relaxation mechanism of highly excited molecular cations.

In Ref. [26], the authors interpreted the observed electron dynamics as a frustrated Auger decay [34] (referred to as shake-up process in Ref. [26]). In their interpretation, the XUV pump ionizes the neutral adenine, creating a cationic species with a vacancy in an inner-valence orbital. The system then undergoes a frustrated decay process in which a valence electron fills the initial vacancy and another one is promoted to a virtual orbital that the authors identify as the 6th orbital above the lowest unoccupied molecular orbital (LUMO), denoted thereafter as LUMO+6. It is supposed that only after that can the NIR probe pulse ionize the electron from the LUMO + 6. The delay in the appearance of the dicationic

---

[*] victor.despre@pci.uni-heidelberg.de
[†] alexander.kuleff@pci.uni-heidelberg.de

signal was therefore interpreted as the time scale of this frustrated decay process, which opens the possibility for ionization with two NIR photons. While formally possible, such a mechanism seems unlikely to be the reason for the observed dynamics. As we will discuss below, in the energy range probed in the experiment, i.e., a few eVs below the double-ionization threshold, the correlation band of the molecule forms, and the notion of individual states and electron configurations ceases to be an adequate description of the system. Due to the strong many-body effects there, the removal of an electron populates a quasicontinuum of cationic states that involve a large number of particle-hole excitations rather than a single, dominant one. In addition, the higher-lying Kohn-Sham virtual orbitals strongly depend on the exchange-correlation functional and the basis set used [35], and thus pinpointing LUMO + 6 as the orbital to which the electron is excited has little physical meaning. For a discussion on the electron-correlation treatment, see also Sec. S6 of the Supplemental Material (SM) [36].

In this Research Letter, we present a different interpretation of the experimental results of Ref. [26], namely, that the observed delay in the appearance of the parent-dication signal is not due to a delayed opening of the second ionization following a frustrated Auger decay process, but to an ultrafast correlation-driven charge migration following the population of the correlation band of adenine that stabilizes the cation. We show that the part of the correlation band that is probed in the experiment is formed by ionization out of four $\sigma$ orbitals, and the subsequent sub-3-fs charge migration represents a redistribution of the charge from a hole with $\sigma$ character to a hole with $\pi$ character. It is the transfer of positive charge from the bonds to an out-of-molecular-plane $\pi$ structure that explains the higher stability of the system after the charge migration and thus the higher probability of creating a stable parent dication. Moreover, we argue that this charge-migration dynamics is not restricted to adenine, but is a general one, to be expected in many molecules following population of their correlation bands. We will also discuss how this charge-migration mechanism can be interpreted in the context of the electron-phonon scattering model used to describe the nonadiabatic dynamics in correlation bands [27].

The starting point for understanding the ultrafast dynamics induced by the pump pulse is the analysis of the ionization spectrum of adenine. To compute the latter, we used the non-Dyson ADC(3) method [37] employing the correlation-consistent polarized, valence-only, double-zeta (cc-pVDZ) basis set. ADC, standing for algebraic diagrammatic construction, is a perturbative method based on the Green's function that provides a high-level *ab initio* description of the electronic structure of an ion and has the advantage of providing all cationic states of the system in a single calculation. We used the third-order ADC scheme [ADC(3)], in which all possible one-hole (1h) and two-holes-one-particle (2h1p) configurations that can be formed within the molecular-orbital basis used are taken into account. This method has been shown to reproduce well the experimental photoelectron spectrum of adenine [38]. The ADC(3)/cc-pVDZ ionization spectrum of adenine is presented in Fig. 1. Each line in the spectrum represents a cationic eigenstate and is located at the corresponding ionization potential. Its height, or spectral intensity, is directly related to the probability of the corresponding state being populated and is given by the 1h part of the state (the total weight of all contributing 1h configurations). As the 2h1p configurations describe excitations on top of the removal of a particular electron, their weight is a measure of the correlation effects contributing to the state.

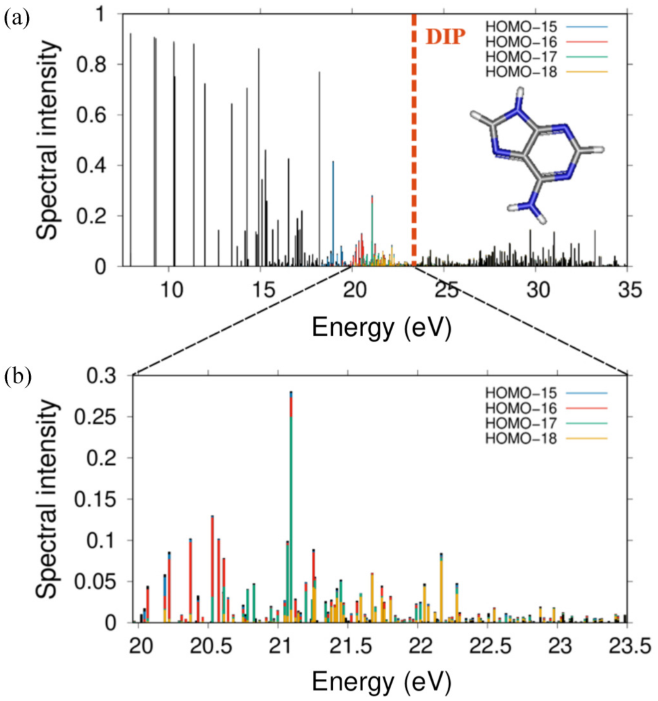

FIG. 1. (a) Ionization spectrum of adenine computed with ADC(3). The dashed orange line, located at 23.5 eV, shows the position of the lowest double-ionization potential (DIP) as reported in Ref. [39]. (b) Zoom of the correlation-band region. The contributions of the one-hole configurations corresponding to the removal of an electron from HOMO − 15, HOMO − 16, HOMO − 17, and HOMO − 18 are depicted with cyan, red, green, and yellow, respectively.

The spectrum of adenine exhibits the typical behavior, with states dominated by 1h configurations at low energy, followed by a region where the multielectronic effects become stronger and many satellite structures appear (between approximately 14 and 18 eV). Above ∼18 eV, we observe a complete breakdown of the molecular-orbital picture, and the spectrum becomes a quasicontinuum of states dominated by multiexcitations—the correlation band of the system. Although the XUV pulse used in Ref. [26] can populate all the states below ∼32 eV, the second ionization performed by the infrared (IR) probe restricts the observed dynamics to the region of the correlation band, located between the double-ionization threshold and a few eVs below it. The double-ionization threshold, denoted in Fig. 1(a) by a dashed orange line, was taken from Ref. [39] and has a value of 23.5 ± 1.0 eV.

Taking a closer look at the correlation-band region of interest [see Fig. 1(b)], we see that it is dominated by states populated by the ionization out of the highest occupied molecular orbital (HOMO) − 16, HOMO − 17, and HOMO − 18, with a smaller contribution from states stemming from ionization of HOMO − 15. All these orbitals are $\sigma$ orbitals. In what follows, we will concentrate on the pure electron dynamics taking place after the ionization of HOMO − 16 as the energy region populated by it correlates best with the observation reported in Ref. [26] that two IR photons of 1.77 eV are needed to further ionize the molecule, noting that the charge migrations triggered by the ionization out of HOMO − 15, HOMO − 17, and HOMO − 18, as well as a combination of the three most important molecular orbitals (HOMO − 16, HOMO − 17, and HOMO − 18), are very similar and can be found in the SM.

The evolution of the electronic cloud following the removal of a HOMO − 16 electron can be traced with the help of the multielectron wave-packet propagation method [9], based on a direct propagation of the initially created electronic wave packet with the full ADC(3) cationic Hamiltonian via the short iterative Lanczos technique [40]. A convenient way to visualize and analyze the dynamics is to compute the hole density, defined as the difference between the electron density of the neutral system, $\rho_0(\vec{r})$, and the time-dependent electron density of the cation, $\rho_i(\vec{r},t)$ [6],

$$Q(\vec{r},t) = \underbrace{\langle\Psi_0|\hat{\rho}|\Psi_0\rangle}_{\rho_0(\vec{r})} - \underbrace{\langle\Phi_i(t)|\hat{\rho}|\Phi_i(t)\rangle}_{\rho_i(\vec{r},t)}, \tag{1}$$

where $|\Psi_0\rangle$ is the neutral ground state, $|\Phi_i(t)\rangle$ is the propagated wave packet created by the ionization at $t = 0$, and $\hat{\rho}$ is the electronic density operator. Using the molecular orbitals of the neutral system as a basis, one can obtain the following expression for the hole density [41]:

$$Q(\vec{r},t) = \sum_p |\tilde{\varphi}_p(\vec{r},t)|^2 \tilde{n}_p(t), \tag{2}$$

where $\tilde{\varphi}_p(\vec{r},t)$ are the natural charge orbitals (given at each time point by different linear combinations of the neutral molecular orbitals) and $\tilde{n}_p(t)$ are their hole-occupation numbers. Further details and the derivation of the above expression can be found in Refs. [9,41,42].

The evolution of the most important hole-occupation numbers following the ionization of HOMO − 16 is shown in Fig. 2 (the hole-occupation numbers following the ionization of HOMO − 18, HOMO − 17, and HOMO − 15 can be found in the SM [36], Figs. S1, S3, and S5, respectively). It is important to note that removing an electron from HOMO − 16 does not mean that a single cationic state is populated. All states, energetically accessible by the pump pulse, with 1h configuration describing an electron missing in HOMO − 16 get populated with the corresponding weights (depicted in red in Fig. 1). An electronic wave packet is thus created by the ionization. We see from Fig. 2 that at time $t = 0$ the hole is in the initially ionized HOMO − 16 orbital. As time progresses, the initial hole is filled (the HOMO − 16 hole occupation decreases), and the hole population is transferred preferentially to orbitals with $\pi$ character (depicted in black in Fig. 2). We note that a negative hole-occupation number means an electron in a virtual natural charge orbital, and thus the hole occupations evolving symmetrically around zero in Fig. 2 describe electronic excitations. The overall dynamics has a time scale of less that 3 fs, in good accord with the observations reported in Ref. [26].

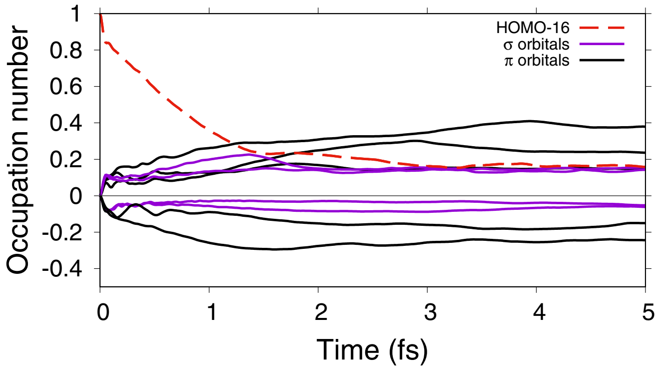

FIG. 2. Evolution of the hole occupations following the removal of an electron from HOMO − 16. A negative hole occupation means that an electron is promoted to a virtual orbital. We see that for time less than 3 fs, the initial hole (red dashed curve) migrates preferentially to $\pi$ orbitals (depicted in black).

To better understand the spatial evolution of the charge during the process, we show in Fig. 3 snapshots of the hole density following ionization out of HOMO − 16 (similar hole density dynamics is observed after the ionization of HOMO − 18, HOMO − 17, and HOMO − 15; see Figs. S2, S4, and S6, respectively, in the SM [36]). At $t = 0$ the hole is located on the imidazole group and, as a consequence of the $\sigma$ character of HOMO − 16, is localized on several bonds. As time progresses, the hole gets delocalized and spreads over the molecule, changing its character from $\sigma$ to $\pi$. As a result of the latter, the positive charge is no longer concentrated on the bonds, but gets localized on the atoms, preferentially outside the molecular plane. It is worth noting that the hole density, being a difference between the total electronic density of the system before and after the ionization [see Eq. (1)], may have regions where an excess of electronic density also builds up. Those are depicted in orange in Fig. 3.

Let us now discuss how the experimental results of Ref. [26] can be interpreted with the help of these correlation-driven charge-migration dynamics. The XUV pump pulse will ionize the system populating all the states below ∼32 eV, but the second ionization by IR probe restricts the observed dynamics to the spectral region spreading just a few eV below the double-ionization threshold. This part of the correlation band of adenine is formed by the ionization out of four orbitals, namely, HOMO − 18 to HOMO − 15. The population of the resulting quasicontinuum of cationic states triggers a sub-3-fs correlation-driven charge-migration dynamics, in which the hole, initially located mostly on the $\sigma$ bonds and thus weakening them, redistributes throughout the system such that at the end of the process it is mostly localized outside the molecular skeleton. In other words, the positive charge that weakens the bond where it is located moves from $\sigma$ to $\pi$ bonds. Due to smaller orbital overlap and the node along the bonding axis, $\pi$ bonds are usually weaker than $\sigma$ bonds [43–45]. This is also confirmed for adenine by the fact that the ground dicationic state is formed by the ionization of two $\pi$ orbitals. This ultrafast charge redistribution therefore

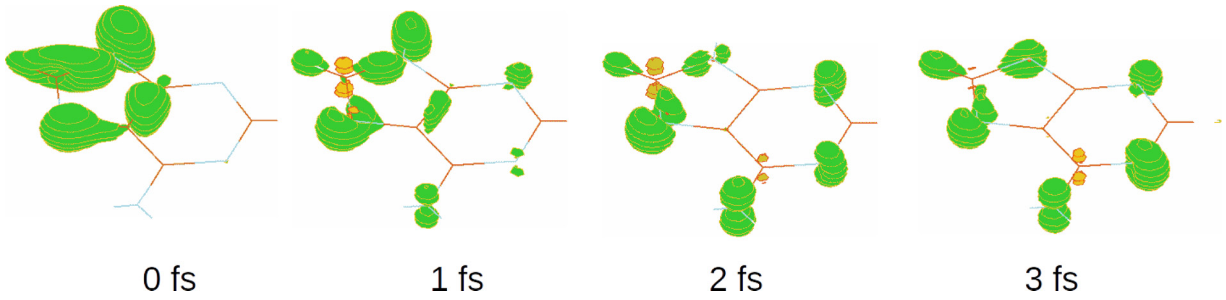

FIG. 3. Snapshot of the hole density at 0, 1, 2, and 3 fs following the removal of an electron from HOMO − 16. Lack of electron density (hole) is depicted in green, while areas with excess electron density are depicted in orange.

stabilizes the cation. If the molecule is further ionized before this stabilization process is completed, the dication is more likely to break apart and thus to contribute to the cationic-fragments signals observed. In contrast, a second ionization performed after the cationic stabilization will increase the probability of observing a stable dicationic system, and thus the parent-dication signal will start to increase. The measured sub-3-fs delay in the appearance of the parent-dication yield is therefore a signature of the correlation-driven charge migration taking place in the correlation band of adenine. The experimental results of Ref. [26] constitute an indirect observation of the discussed mechanism. It might be directly accessible, for example, with time-resolved photoelectron spectroscopy [46,47]. The shape of the measured delayed XUV+NIR photoelectron signal, broad (correlation band) or narrow (single decaying state), will also help in identifying the observed mechanism.

Let us now discuss our results in a broader context. While the delay observed in the dicationic signal of adenine could be specific to this molecule, the correlation-driven charge migration triggered by the population of the correlation band is a general effect. Indeed, correlation bands are formed in the cationic spectra of every polyatomic molecule, and thus the removal of an electron from deep inner-valence orbitals will inevitably lead to the population of a quasicontinuum of states spread over, sometimes, several eV. Such an electronic wave packet will evolve on an ultrashort time scale (a few femtoseconds) redistributing the charge throughout the system and preparing it for the follow-up nonadiabatic dynamics. The correlation-driven charge-migration process will therefore serve as an initial step in the relaxation in the correlation band. Due to the large number of states involved, a full treatment of the electron-nuclear dynamics occurring in a correlation band, from the correlation-driven charge migration to the subsequent energy redistribution between electronic and nuclear degrees of freedom, is currently out of reach. It is thus necessary to develop models that can provide a qualitative, and, if possible, quantitative, physical picture. In the following we will briefly discuss a promising pathway.

It was recently shown [27] that the nonadiabatic relaxation dynamics in the correlation band of whole classes of molecules can be modeled and understood with the help of a simple electron-phonon scattering model used to describe losses in conduction bands of solids. Extending the analogy between correlation bands in molecules and energy bands in solids introduced in Ref. [27], the correlation-driven charge migration can be seen as being equivalent to the electron cooling occurring through electron-electron collisions in solids. In both cases, the energy is first localized on a specific part of the system and then, due only to the electron correlation, efficiently spreads over the system. The development of such models might offer a new perspective in the understanding of the physics of correlation bands and the relaxation of highly excited molecular cations.

Finally, we would like to touch upon the possible consequences of such a sequence of ultrafast processes initiated by the ionization of a molecule with XUV light. Following the concept of attochemistry [48], the possibility to exert control over the initial, pure electronic charge-redistribution step can be used to modulate the follow-up relaxation dynamics and thus the chemical reactivity of the molecule, eventually influencing the fragmentation pattern. Efficient control over charge-migration dynamics has already been demonstrated theoretically in the outer valence [49,50], where typically only several states participate. The extension of these techniques to dense spectral regions and the development of new ones might offer interesting perspectives in quantum control of photoinduced chemistry and a deeper understanding of the radiation damage in (bio)matter.

The authors thank Nikolay Golubev for valuable discussions and technical support with the multielectron wave-packet propagation code and acknowledge financial support from the DFG through the QUTIF priority program.

[1] M. Nisoli, P. Decleva, F. Calegari, A. Palacios, and F. Martín, Chem. Rev. (Washington, DC) **117**, 10760 (2017).

[2] F. Calegari, D. Ayuso, A. Trabattoni, L. Belshaw, S. De Camillis, S. Anumula, F. Frassetto, L. Poletto, A. Palacios, P. Decleva, J. B. Greenwood, F. Martín, and M. Nisoli, Science **346**, 336 (2014).

[3] P. M. Kraus, B. Mignolet, D. Baykusheva, A. Rupenyan, L. Horny, E. F. Penka, G. Grassi, O. I. Tolstikhin, J. Schneider, F. Jensen, L. B. Madsen, A. D. Bandrauk, F. Remacle, and H. J. Wörner, Science **350**, 790 (2015).

[4] M. Lara-Astiaso, M. Galli, A. Trabattoni, A. Palacios, D. Ayuso, F. Frassetto, L. Poletto, S. De Camillis, J. Greenwood,

P. Decleva, I. Tavernelli, F. Calegari, M. Nisoli, and F. Martín, J. Phys. Chem. Lett. **9**, 4570 (2018).
[5] F. Remacle, R. Levine, and M. A. Ratner, Chem. Phys. Lett. **285**, 25 (1998).
[6] L. S. Cederbaum and J. Zobeley, Chem. Phys. Lett. **307**, 205 (1999).
[7] H. Hennig, J. Breidbach, and L. S. Cederbaum, J. Phys. Chem. A **109**, 409 (2005).
[8] G. L. Yudin, S. Chelkowski, J. Itatani, A. D. Bandrauk, and P. B. Corkum, Phys. Rev. A **72**, 051401(R) (2005).
[9] A. I. Kuleff, J. Breidbach, and L. S. Cederbaum, J. Chem. Phys. **123**, 044111 (2005).
[10] I. Barth and J. Manz, Angew. Chem. Int. Ed. **45**, 2962 (2006).
[11] A. I. Kuleff, S. Lünnemann, and L. S. Cederbaum, J. Phys. Chem. A **114**, 8676 (2010).
[12] T. Kuś, B. Mignolet, R. D. Levine, and F. Remacle, J. Phys. Chem. A **117**, 10513 (2013).
[13] M. Lara-Astiaso, D. Ayuso, I. Tavernelli, P. Decleva, A. Palacios, and F. Martín, Faraday Discuss. **194**, 41 (2016).
[14] S. Sun, B. Mignolet, L. Fan, W. Li, R. D. Levine, and F. Remacle, J. Phys. Chem. A **121**, 1442 (2017).
[15] F. Mauger, P. M. Abanador, A. Bruner, A. Sissay, M. B. Gaarde, K. Lopata, and K. J. Schafer, Phys. Rev. A **97**, 043407 (2018).
[16] V. Despré and A. I. Kuleff, Theor. Chem. Acc. **138**, 110 (2019).
[17] E. Perfetto, A. Trabattoni, F. Calegari, M. Nisoli, A. Marini, and G. Stefanucci, J. Phys. Chem. Lett. **11**, 891 (2020).
[18] D. Schwickert, M. Ruberti, P. Kolorenč, S. Usenko, A. Przystawik, K. Baev, I. Baev, M. Braune, L. Bocklage, M. K. Czwalinna, S. Deinert, S. Düsterer, A. Hans, G. Hartmann, C. Haunhorst, M. Kuhlmann, S. Palutke, R. Röhlsberger, J. Rönsch-Schulenburg, P. Schmidt *et al.*, Sci. Adv. **8**, eabn6848 (2022).
[19] A. S. Folorunso, A. Bruner, F. Mauger, K. A. Hamer, S. Hernandez, R. R. Jones, L. F. DiMauro, M. B. Gaarde, K. J. Schafer, and K. Lopata, Phys. Rev. Lett. **126**, 133002 (2021).
[20] A. I. Kuleff and L. S. Cederbaum, J. Phys. B: At. Mol. Opt. Phys. **47**, 124002 (2014).
[21] V. Despré, A. Marciniak, V. Loriot, M. C. E. Galbraith, A. Rouzée, M. J. J. Vrakking, F. Lépine, and A. I. Kuleff, J. Phys. Chem. Lett. **6**, 426 (2015).
[22] M. Vacher, L. Steinberg, A. J. Jenkins, M. J. Bearpark, and M. A. Robb, Phys. Rev. A **92**, 040502(R) (2015).
[23] M. Vacher, M. J. Bearpark, M. A. Robb, and J. P. Malhado, Phys. Rev. Lett. **118**, 083001 (2017).
[24] C. Arnold, O. Vendrell, and R. Santra, Phys. Rev. A **95**, 033425 (2017).
[25] V. Despré, N. V. Golubev, and A. I. Kuleff, Phys. Rev. Lett. **121**, 203002 (2018).
[26] E. P. Månsson, S. Latini, F. Covito, V. Wanie, M. Galli, E. Perfetto, G. Stefanucci, H. Hübener, U. De Giovannini, M. C. Castrovilli, A. Trabattoni, F. Frassetto, L. Poletto, J. B. Greenwood, F. Légaré, M. Nisoli, A. Rubio, and F. Calegari, Commun. Chem. **4**, 73 (2021).
[27] M. Hervé, V. Despré, P. Castellanos Nashn, V. Loriot, A. Boyer, A. Scognamiglio, G. Karras, R. Brédy, E. Constant, A. G. G. M. Tielens, A. I. Kuleff, and F. Lépine, Nat. Phys. **17**, 327 (2021).
[28] L. Belshaw, F. Calegari, M. J. Duffy, A. Trabattoni, L. Poletto, M. Nisoli, and J. B. Greenwood, J. Phys. Chem. Lett. **3**, 3751 (2012).
[29] A. Marciniak, V. Despré, T. Barillot, A. Rouzée, M. C. E. Galbraith, J. Klei, C.-H. Yang, C. T. L. Smeenk, V. Loriot, S. N. Reddy, A. G. G. M. Tielens, S. Mahapatra, A. I. Kuleff, M. J. J. Vrakking, and F. Lépine, Nat. Commun. **6**, 7909 (2015).
[30] A. Marciniak, K. Yamazaki, S. Maeda, M. Reduzzi, V. Despré, M. Hervé, M. Meziane, T. A. Niehaus, V. Loriot, A. I. Kuleff, B. Schindler, I. Compagnon, G. Sansone, and F. Lépine, J. Phys. Chem. Lett. **9**, 6927 (2018).
[31] M. S. Deleuze and L. S. Cederbaum, Phys. Rev. B **53**, 13326 (1996).
[32] L. S. Cederbaum, W. Domcke, J. Schirmer, and W. Von Niessen, in *Advances in Chemical Physics Volume 65* (Wiley, New York, 1986), pp. 115–159.
[33] A. Boyer, M. Hervé, V. Despré, P. Castellanos Nash, V. Loriot, A. Marciniak, A. G. G. M. Tielens, A. I. Kuleff, and F. Lépine, Phys. Rev. X **11**, 041012 (2021).
[34] P. S. Bagus, R. Broer, and E. S. Ilton, Chem. Phys. Lett. **394**, 150 (2004).
[35] R. van Meer, O. V. Gritsenko, and E. J. Baerends, J. Chem. Theor. Comput. **10**, 4432 (2014).
[36] See Supplemental Material at http://link.aps.org/supplemental/10.1103/PhysRevA.106.L021501 for an analysis of the dynamics resulting from the ionization of HOMO − 18, HOMO − 17, and HOMO − 15 and a mixture of HOMO − 18, HOMO − 17, and HOMO − 16.
[37] J. Schirmer, A. B. Trofimov, and G. Stelter, J. Chem. Phys. **109**, 4734 (1998).
[38] A. Trofimov, J. Schirmer, V. Kobychev, A. Potts, D. Holland, and L. Karlsson, J. Phys. B: At. Mol. Opt. Phys. **39**, 305 (2006).
[39] P. J. van der Burgt, S. Finnegan, and S. Eden, Eur. Phys. J. D **69**, 173 (2015).
[40] T. J. Park and J. C. Light, J. Chem. Phys. **85**, 5870 (1986).
[41] J. Breidbach and L. Cederbaum, J. Chem. Phys. **118**, 3983 (2003).
[42] J. Breidbach and L. Cederbaum, J. Chem. Phys. **126**, 034101 (2007).
[43] L. Pauling, *The Nature of the Chemical Bond* (Cornell University Press, Ithaca, NY, 1960).
[44] M. W. Schmidt, P. N. Truong, and M. S. Gordon, J. Am. Chem. Soc. **109**, 5217 (1987).
[45] D. J. Grant and D. A. Dixon, J. Phys. Chem. A **110**, 12955 (2006).
[46] M. Eckstein, C.-H. Yang, F. Frassetto, L. Poletto, G. Sansone, M. J. J. Vrakking, and O. Kornilov, Phys. Rev. Lett. **116**, 163003 (2016).
[47] A. Marciniak, V. Despré, V. Loriot, G. Karras, M. Hervé, L. Quintard, F. Catoire, C. Joblin, E. Constant, A. Kuleff, and F. Lépine, Nat. Commun. **10**, 337 (2019).
[48] A. Palacios and F. Martín, WIREs Comput. Mol. Sci. **10**, e1430 (2020).
[49] N. V. Golubev and A. I. Kuleff, Phys. Rev. A **91**, 051401(R) (2015).
[50] N. V. Golubev, V. Despré, and A. I. Kuleff, J. Mod. Opt. **64**, 1031 (2017).